1   **The Tension-sensitive Ion Transport Activity of MSL8 is Critical for its Function in Pollen**

2   **Hydration and Germination**

3

4   Running title:

5   Ion transport is required for MSL8 pollen function

6

7   Corresponding author: Dr. E. S. Haswell

8   Department of Biology, Box 1137, Washington University in St. Louis, 1 Brookings Drive, Saint Louis, MO,

9   63130, USA.

10   314-935-9223

11   ehaswell@wustl.edu

12

13   Subject areas: growth and development; membrane and transport

14

15   1 black and white figure; 7 color figures; 3 tables; 4 supplementary figures and 4 supplementary tables

16

17 **The Tension-sensitive Ion Transport Activity of MSL8 is Critical for its Function in Pollen**

18 **Hydration and Germination**

19

20 Running title:

21 Ion transport is required for MSL8 pollen function

22

23 Eric S. Hamilton and Elizabeth S. Haswell

24 Department of Biology, Box 1137, Washington University in St. Louis, 1 Brookings Drive, Saint Louis, MO,

25 63130, USA.

26

27 Abbreviations: cRNA, capped RNA; MS, mechanosensitive; MscL, Mechanosensitive channel of Large

28 conductance; MscS, Mechanosensitive channel of Small conductance; MSL8, MscS-Like 8; MSL10;

29 MscS-Like 10; PEG, polyethylene glycol; TM, transmembrane

30

31   **Abstract**

32   All cells respond to osmotic challenges, including those imposed during normal growth and development.

33   Mechanosensitive (MS) ion channels provide a conserved mechanism for regulating osmotic forces by

34   conducting ions in response to increased membrane tension. We previously demonstrated that the MS

35   ion channel MscS-Like 8 (MSL8) is required for pollen to survive multiple osmotic challenges that occur

36   during the normal process of fertilization, and that it can inhibit pollen germination. However, it remained

37   unclear whether these physiological functions required ion flux through a mechanically gated channel

38   provided by MSL8. We introduced two point mutations into the predicted pore-lining domain of MSL8 that

39   disrupted normal channel function in different ways. The Ile711Ser mutation increased the tension

40   threshold of the MSL8 channel while leaving conductance unchanged, and the Phe720Leu mutation

41   severely disrupted the MSL8 channel. Both of these mutations impaired the ability of MSL8 to preserve

42   pollen viability during hydration and to maintain the integrity of the pollen tube when expressed at

43   endogenous levels. When overexpressed in a *msl8-4* null background, MSL8^{I711S} could partially rescue

44   loss-of-function phenotypes, while MSL8^{F720L} could not. When overexpressed in the wild type L*er*

45   background, MSL8^{I711S} suppressed pollen germination, similar to wild type MSL8. In contrast, MSL8^{F720L}

46   failed to suppress pollen germination and increased pollen bursting, thereby phenocopying the *msl8-4*

47   mutant. Thus, an intact MSL8 channel is required to for normal pollen function during hydration and

48   germination. These data establish MSL8 as the first plant MS channel to fulfill previously established

49   criteria for assignment as a mechanotransducer.

50

53

54 **Introduction**

55 In order to thrive, all cells must respond to osmotic challenges. Drought, salt stress, and freezing all

56 present environmentally imposed stresses that require osmoprotective strategies for cell survival (Burg

57 and Ferraris, 2008; Zhang, 1999). Organisms can also experience osmotic challenges inherent to their

58 growth and development, such as desiccation during endospore formation in response to stress (Tovar-

59 Rojo et al., 2003), the transition from seawater to saltwater experienced by migrating salmon (Jeffries et

60 al., 2011), or drying and rehydration of plant seeds (Hoekstra et al., 2001).

61

62 One conserved molecular mechanism for responding to osmotic challenges and other mechanical stimuli

63 is the use of mechanosensitive (MS) ion channels (Booth and Blount, 2012; Hamilton et al., 2015b;

64 Ranade et al., 2015). These proteins form pores in the cell membrane that open in response to

65 mechanical stimulation, allowing ions to flow across the membrane down their electrochemical gradient. A

66 role for MS ion channels in osmotic regulation has been well described in *Escherichia coli*, where the

67 Mechanosensitive channel of Large conductance (MscL) and Mechanosensitive channel of Small

68 conductance (MscS) are required for the cell to survive extreme hypoosmotic downshock, such as the

69 transfer from 500 mM NaCl to distilled water (Levina et al., 1999). It is proposed that when cells are

70 exposed to hypoosmotic shock, the resultant cell swelling and increase in membrane tension increase the

71 open probability of both MscS and MscL. When open, these channels allow osmolytes to flow out of the

72 cell, reducing internal osmotic pressure and protecting the bacterium from lysis (Booth and Blount, 2012;

73 Kung et al., 2010). Thus, bacterial MS ion channels are often referred to as osmotic pressure release

74 valves.

75

76 *Ec*MscS is the founding member of a large family of conserved proteins found within prokaryotes,

77 archaea, and many eukaryotes, including plants (Haswell, 2007; Kloda and Martinac, 2002; Koprowski

78 and Kubalski, 2003; Levina et al., 1999; Malcolm and Maurer, 2012; Pivetti et al., 2003; Porter et al.,

79 2009; Prole and Taylor, 2013). Crystal structures of MscS homologs from *E. coli* and *Helicobacter pylori*

80 have shown that these proteins form homoheptamers (Bass et al., 2002; Lai et al., 2013; Steinbacher et

81   al., 2007; Wang et al., 2008), but no structural information yet exists for eukaryotic MscS family members.

82   Ten MscS homologs are encoded in the *Arabidopsis thaliana* genome, named MscS-Like (MSL) 1-10

83   (Haswell, 2007). MSL proteins localize to diverse cell compartments, including the mitochondria (Lee et

84   al., 2016), plastids (Haswell and Meyerowitz, 2006), and the plasma membrane (Hamilton et al., 2015a;

85   Haswell et al., 2008; Veley et al., 2014).

86

87   We recently showed that plasma membrane-localized MSL8 is required to protect pollen from osmotic

88   challenges during several steps in fertilization (Hamilton et al., 2015a). Pollen contains the male gametes

89   of flowering plants and is responsible for the delivery of two sperm cells to the female gametophyte in

90   order to produce the next generation (Hafidh et al., 2016). During key steps of desiccation, rehydration,

91   germination, and tube growth, pollen must regulate its osmotic potential to maintain the integrity of the cell

92   and achieve its reproductive function (Beauzamy et al., 2014; Chen et al., 2015; Feijo et al., 1995; Firon

93   et al., 2012; Sanati Nezhad et al., 2013).

94

95   Upon maturation, the pollen of most species of flowering plants desiccates (Franchi et al., 2011), a

96   strategy thought to maintain viability during exposure to the external environment (Firon et al., 2012). To

97   protect against the osmotic stress of this water loss, pollen accumulates sugars and other compatible

98   osmolytes that serve to stabilize cellular membranes and other biomolecules in the dry state (Hoekstra et

99   al., 2001; Pacini et al., 2006). When a desiccated pollen grain reaches the stigma, an organ of finger-like

100   projections atop the pistil, it is rehydrated by stigma cell exudate in a regulated process of pollen

101   reception (Dresselhaus and Franklin-Tong, 2013; Edlund, 2004; Samuel et al., 2009). The stigma exudate

102   of Lily, which has a wet stigma coated in exudate, is more than 90% water, with carbohydrates making up

103   the majority of the solutes (Labarca et al., 1970). The composition of the exudate produced in species

104   with dry stigmas, such as Arabidopsis, is unknown (Edlund, 2004), but must be hypoosmotic with respect

105   to the pollen cytoplasm in order to produce net hydration. The rehydration of desiccated pollen can

106   damage dry cellular membranes, which are more rigid and less able to accommodate hypoosmotic

107   swelling (Hoekstra et al., 2001; 1997), and this membrane damage can compromise pollen viability if

108   hydration is not properly regulated (van Bilsen et al., 1994).

109

110   Once a pollen grain is rehydrated, its metabolism is reactivated and it germinates a long extension that

111   grows by turgor-driven cell expansion at the tip without further cell divisions, called a pollen tube

112   (Beauzamy et al., 2014; Firon et al., 2012). Germination requires that the pollen grain establish and

113   maintain turgor pressure at a level high enough to break through the tough pollen cell wall (Feijo et al.,

114   1995). The rapid growth of the pollen tube is also driven by turgor pressure, which continuously expands

115   new cell wall material delivered to the growing tip (Hill et al., 2012; Kroeger et al., 2011; Zerzour et al.,

116   2009). Artificially increasing turgor pressure can lead to lysis, especially at the tip of the pollen tube

117   (Benkert et al., 1997), and genetic lesions that increase turgor impair the ability of the pollen tube to reach

118   the ovule and fertilize the egg cell (Chen et al., 2015). Conversely, growth conditions that reduce turgor

119   halt pollen tube growth (Zerzour et al., 2009). In addition to turgor, pollen tubes must regulate the delivery

120   of new cell wall material and cell wall composition in order to sustain growth while maintaining the

121   integrity of the cell (Hill et al., 2012; Kroeger et al., 2011; Zerzour et al., 2009). These observations have

122   led to the proposal that pollen grains utilize a mechanosensor to respond to changes in osmotic potential

123   (Hill et al., 2012), and a role for MS ion channels in regulating ion fluxes at the dynamic pollen tube tip

124   has been proposed for decades (Feijo et al., 1995).

125

126   MSL8 provides one mechanism for regulating these osmotic forces in pollen. Both loss of function

127   mutations in the *MSL8* gene and *MSL8* overexpression result in male fertility defects, indicating that the

128   proper expression level of *MSL8* is essential for full reproductive success (Hamilton et al., 2015a). Two

129   independent T-DNA insertion alleles, the partial loss-of-function *msl8-1* in the Col-*0* background and the

130   null *msl8-4* in the L*er* background, result in reduced viability when pollen is hydrated in distilled water.

131   This hydration viability defect can be rescued by supplementing hydration media with a 20% solution of

132   polyethylene glycol (PEG); increasing the osmotic potential of the media reduces the hypoosmotic shock

133   pollen experiences during hydration. Expression of *MSL8-GFP* from genomic sequences fully

134   complements this reduced viability during *in vitro* hydration in both allele backgrounds. MSL8 also

135   negatively regulates pollen germination while maintaining the integrity of germinating pollen tubes. Mutant

136   *msl8* pollen germinates at a greater rate than wild type pollen, but bursts more frequently. Overexpressing

137   *MSL8* in the L*er* background strongly suppresses pollen germination, which leads to reduced fertility.

138

139   Thus, MSL8 is required to protect pollen against excessive osmotic pressure, either during rehydration or

140   during the turgor-driven germination and growth of a pollen tube. Because MSL8 forms a MS ion channel,

141   we hypothesized that the flow of ions through the MSL8 pore in response to increases in membrane

142   tension is critical for preventing lysis during hydration and germination, akin to the function of MscS in *E.*

143   *coli.* However, it remained possible that the role of MSL8 in pollen survival is indirect. Indeed, close

144   homolog MSL10 triggers programmed cell death signaling independent of its channel activity (Veley et al.,

145   2014).

146

147   Here we report the results of experiments aimed to determine if MSL8 requires an intact channel to

148   achieve its function in pollen. To do so, we mutated the predicted pore of the MSL8 channel, identified

149   lesions that affect channel behavior, and analyzed the ability of these mutants to function in pollen. Our

150   results support a model wherein MSL8 regulates osmotic forces in pollen directly by transporting ions.

151

152   **Results**

153   *Mutations in the predicted pore-lining domain of MSL8 alter its channel properties*

154   In order to alter the channel properties of MSL8, we identified candidate amino acids for mutagenesis

155   based alignment with *Ec*MscS. The predicted topology of a MSL8 monomer shown in Fig. 1A indicates a

156   protein with 6 transmembrane (TM) helices and three soluble domains. The most C-terminal TM helix,

157   TM6, contains sequence with modest homology to the pore-lining TM3 of *Ec*MscS (marked with a thick

158   line in Fig. 1A and sequence shown in Fig. 1B).

159

160   In the *Ec*MscS channel, Leu105 and Leu109 from each of the seven monomers are proposed to form a

161   hydrophobic seal in the closed channel that prevents the flow of ions across the pore (Anishkin and

162   Sukharev, 2004; Bass et al., 2002; Steinbacher et al., 2007) (arrowheads, Fig. 1B). Mutations in nearby

163   residues can result in decreased tension sensitivity, increased tension sensitivity, or reduced

164   conductance (Belyy et al., 2010; Edwards et al., 2005; Rasmussen et al., 2015). To create MSL8 variants

165   with altered channel properties, we replaced hydrophobic residues surrounding the presumptive

166   hydrophobic seal with polar residues or smaller non-polar residues. Two mutants, Ile711 to Ser and

167   Phe720 to Leu (asterisks, Fig. 1B) were selected for further study based on their ability to produce MS

168   currents when expressed in *Xenopus laevis* oocytes (see below).

169

170   *MSL8*, *MSL8^{I711S}* and *MSL8^{F720L}* cRNAs were injected into *Xenopus* oocytes for analysis by single

171   channel patch-clamp electrophysiology as previously described (Hamilton et al., 2015a; Maksaev and

172   Haswell, 2015). Patches of plasma membrane were excised from oocytes 2 to 10 days after injection, and

173   current measured over time as membrane tension in the patch was increased by applying suction through

174   the pipette using a pressure-clamp controller. In symmetric 60 mM $MgCl_2$ + 5mM HEPES, oocytes

175   expressing wild type *MSL8* cRNA exhibited tension-gated activity as expected (Fig. 1C, top left panel), as

176   did oocytes injected with *MSL8^{I711S}* cRNA (Fig. 1C, top right panel). In the same system, *MSL8^{F720L}* cRNA

177   produced MS currents without discrete channel openings (Fig. 1C, bottom left panel; see Supplementary

178   Fig. S1 for more examples of activity associated with *MSL8^{F720L}* cRNA), and no currents were observed in

179   water-injected oocytes (Fig. 1C, bottom right panel). MS currents were observed in 23 of 26 patches

180   pulled from oocytes injected with *MSL8* cRNA; 27 of 32 patches for *MSL8^{I711S}*; 20 out of 24 patches for

181   *MSL8^{F720L}*; and in none of 26 patches from water-injected oocytes (Table 1). Under these conditions, the

182   single-channel conductance of MSL8^{I711S} was indistinguishable from that of wild type MSL8 (Fig. 1D,

183   Table 1). Without distinguishable individual gating events, we were unable to assess the single channel

184   conductance of MSL8^{F720L}.

185

186   We were unable to calculate a midpoint gating tension, because membrane patches ruptured before

187   current saturation, as previously observed for MSL10 expressed in *Xenopus* oocytes (Maksaev and

188   Haswell, 2012). Instead, we estimated the tension sensitivity of each MSL8 variant, by recording the

189   suction associated with the opening of the first channel and the closing of the last channel in each patch.

190   Patch pipettes of size 3 ± 0.5 MOhm were used in all experiments to reduce variability in patch geometry.

191   The negative pressure required to open the first channel in patches expressing wild type MSL8 was -18.0

192      $\pm$ 13.1 mmHg, while for MSL8^{I711S} it was -29.5 $\pm$ 11.7 mmHg (Table 1). While we were unable to identify

193   discrete channel openings for MSL8^{F720L}, we estimated its tension threshold by determining the pressure

194   required to produce visible MS currents, on average -61.2 $\pm$ 12.3 mmHg (Table 1). In summary, MSL8^{I711S}

195   had the same conductance as wild type MSL8, but was significantly less tension-sensitive (required

196   greater negative pressure to open). MSL8^{F720L} appears to be a severely disrupted channel, albeit one

197   capable of conducting ions through its pore in response to extremely high membrane tension,

198   approximately 3 times higher than that required to open wild type MSL8.

199

200   *MSL8 channel mutants do not complement msl8-4 mutant phenotypes when expressed from genomic*

201   *sequences.*

202   To determine whether channel activity was required for MSL8 to protect pollen from osmotic challenges,

203   we tested whether MSL8^{I711S} or MSL8^{F720L} could complement previously characterized *msl8-4* mutant

204   defects. MSL8, MSL8^{I711S} and MSL8^{F720L} were tagged with GFP at the C-terminus and expressed from

205   genomic sequences in the null *msl8-4* mutant background. The wild type version of this transgene,

206   termed *gMSL8-GFP*, was shown to rescue the *in vitro* hydration viability defect of *msl8-4* pollen (Hamilton

207   et al., 2015a). Lines expressing wild type and mutant versions of *gMSL8-GFP* were generated and

208   screened for expression of *MSL8* variants in floral RNA. Two independent homozygous transgenic lines

209   expressing *gMSL8^{I711S}-GFP* or *gMSL8^{F720L}-GFP* and a single control line expressing wild type *gMSL8-*

210   *GFP* were selected for further analysis. All lines selected accumulated *MSL8* transcripts at levels equal to

211   or greater than the wild-type L*er* (Fig. 2A). To confirm protein production, stability and subcellular

212   localization, confocal images were taken of GFP signal in mature, desiccated pollen isolated from these

213   lines. All five lines expressing *gMSL8-GFP* or variants in the *msl8-4* background exhibited GFP signal

214   localized to both the plasma membrane and endomembrane compartments and excluded from vacuoles,

215   as previously observed for MSL8-GFP (Fig. 2B; (Hamilton et al., 2015a). Untransformed *msl8-4* mutant

216   pollen only exhibited autofluorescence of the cell wall.

217

218   To test the ability of MSL8^{I711S} and MSL8^{F720L} to protect *msl8-4* pollen from the hypoosmotic shock of

219   rehydration, we quantified the viability of mature, desiccated pollen after rehydration in distilled water. In a

220   rehydration time course from 30 to 120 minutes, As expected, L*er* pollen viability exceeded 80% at all

221   time points, while *msl8-4* pollen exhibited less than 35% survival on average, and *msl8-4* pollen

222   expressing wild type *gMSL8-GFP* exhibited wild-type survival at all time points (Fig. 3A). However, there

223   were no differences between the viability of *msl8-4* pollen and *msl8-4* pollen expressing the *gMSL8^{I711S}-*

224   *GFP* or *gMSL8^{F720L}-GFP* transgenes in water at 30, 60, or 120 minutes after hydration. Thus, neither

225   MSL8^{I711S} nor MSL8^{F720L} could complement this *msl8-4* mutant phenotype.

226

227   To determine if MSL8^{I711S} or MSL8^{F720L} could protect *msl8-4* pollen from intermediate levels of

228   hypoosmotic stress, we quantified pollen viability following a 30-minute incubation in a range of PEG$_{3350}$

229   concentrations. Supplementing hydration media with 15% PEG$_{3350}$ increased the average viability of

230   *msl8-4* pollen from 30% to 79% (Fig. 3B). PEG supplementation also increased the survival rate of *msl8-4*

231   pollen expressing *gMSL8^{I711S}-GFP* and *gMSL8^{F720L}-GFP*, to a degree that was indistinguishable from that

232   of the mutant *msl8-4* pollen across all levels of PEG (Fig. 3B). Thus, the *gMSL8^{I711S}-GFP* and

233   *gMSL8^{F720L}-GFP* transgenes did not alter the sensitivity of *msl8-4* pollen to rehydration, even when

234   osmotic supplementation was used to reduce the severity of the osmotic downshock.

235

236   *msl8-4* pollen survives hydration in germination media, as it contains osmolytes (580 mOsmol), but

237   exhibits increased germination rates and pronounced bursting when germinated *in vitro* (Hamilton et al.,

238   2015a). We therefore quantified the germination and bursting rates of *msl8-4* pollen expressing

239   *gMSL8^{I711S}-GFP-* and *gMSL8^{F720L}-GFP*. After incubation in germination media for 6 hours, most L*er* pollen

240   was ungerminated and intact; 8% was ungerminated and burst; 12% germinated and was intact; and 4%

241   germinated and burst (Fig. 4, Supplementary Table S1). *msl8-4* pollen germinated at a similar rate to L*er*,

242   but 37% of ungerminated mutant pollen grains burst. Most of the *msl8-4* pollen that did germinate went on

243   to burst, leaving only 49% intact pollen (compared to 89% for the wild type). While *msl8-4* pollen

244   expressing *gMSL8-GFP* barely germinated or burst at all (< 0.5%) under these conditions, pollen

245   expressing *gMSL8^{I711S}-GFP* or *gMSL8^{F720L}-GFP* had germination and bursting rates similar to *msl8-4*

246   pollen. We thus found no evidence that MSL8^{I711S} or MSL8^{F720L} could substantially rescue known *msl8-4*

247   loss-of-function phenotypes (Figs. 3-4), even though these variants were expressed at or above native

248   levels and localized normally (Fig. 2).

249

250   *MSL8^{I711S} but not MSL8^{F720L} partially rescues msl8-4 loss-of-function phenotypes when overexpressed.*

251   To determine if we could detect partially functional channels if they were present at high levels, MSL8,

252   MSL8^{I711S} or MSL8^{F720L} were tagged at the C-terminus with YFP and expressed under the control of the

253   strong, pollen-specific promoter *LAT52* in the *msl8-4* background. We identified multiple independent

254   homozygous lines that exhibited a range of transgene expression levels in floral RNA, from 1.9- to 9.6-

255   fold over the levels of endogenous *MSL8* in L*er* (Fig. 5A). YFP signal in *msl8-4* pollen expressing

256   *LAT52pMSL8-YFP* and variants localized to the plasma membrane and endomembrane compartments of

257   mature pollen (Fig. 5B; Supplementary Fig. S2A), and the intensity of YFP signal correlated with transcript

258   level as revealed by RT-PCR (compare Fig. 5A and Supplementary Fig. S2A).

259

260   Pollen from L*er* and *msl8-4* lines overexpressing MSL8, MSL8^{I711S}, and MSL8^{F720L} was incubated in

261   distilled water for 30 or 120 minutes and viability quantified as in Fig. 3. All three *msl8-4 + LAT52pMSL8-*

262   *YFP* lines survived as well as wild-type pollen at both time points, while the viability of *msl8-4* pollen

263   expressing *LAT52pMSL8^{F720L}-YFP* was indistinguishable from that of *msl8-4* in all three independent lines

264   (Fig. 6). Thus, even at high levels of expression, *MSL8^{F720L}* was unable to protect pollen from the

265   hypoosmotic shock of rehydration. However, pollen from three *msl8-4 + LAT52pMSL8^{I711S}-YFP* lines

266   exhibited intermediate levels of pollen viability when hydrated in water. The level of protection was

267   correlated with the level of *MSL8^{I711S}* expression in each line. Two independent lines, I711S-7 and I711S-

268   12, exhibited averages of 44% to 63% survival during the time course. At both time points, I711S-7- and

269   I711S-12 pollen viability was statistically significantly different from L*er*, *msl8-4*, and the other transgenic

270   lines, representing an intermediate phenotype. The strongest-expressing line, I711S-4 (Fig. 5A), exhibited

271   wild-type pollen viability at both 30 and 120 minutes. Thus, MSL8^{I711S} is able to partially rescue the *msl8-4*

272   hydration viability defect when moderately overexpressed, while sufficiently high levels of expression fully

273   complement the mutant phenotype.

274

275   Next, we incubated pollen from *msl8-4 + LAT52pMSL8-YFP* and variant lines in germination media for 6

276   hours and quantified germination and bursting rates (Fig. 7A). As expected, expression of *LAT52pMSL8-*

277   *YFP* suppressed both germination and bursting rates of *msl8-4*, to less than 1%, while expression of

278   *LAT52pMSL8^{F720L}-YFP* did not (Fig. 7A, Supplementary Table S2). As with pollen rehydration,

279   overexpression of *MSL8^{I711S}* in the *msl8-4* background resulted in partial rescue of the loss-of-function

280   phenotypes. Mutant pollen expressing *LAT52pMSL8^{I711S}-YFP* germinated an average of 0% to 17%, and

281   burst on average 4% to 36% of the time (much lower than the approximately 25% germination and 50%

282   bursting of *msl8-4*). Both germination and bursting rates were inversely correlated to the level of *MSL8*

283   accumulation in the *LAT52pMSL8^{I711S}-YFP* line (compare Figs. 5A and 7A). The pattern of bursting and

284   germination in the highest expressing line, I711S-4, was statistically indistinguishable from line WT-11

285   (Supplementary Table S2), indicating that MSL8^{I711S} can fully complement when highly overexpressed.

286

287   Because germination is suppressed so strongly by *MSL8* overexpression, we also incubated pollen in

288   germination media for an extended period of time (overnight, or 16 hours), in order to maximize the

289   number of germination events (Fig. 7B-C, Supplementary Fig. S2B). Under these conditions, 63% of

290   *msl8-4* pollen germinated on average, compared to 44% of L*er* pollen. The overexpression of *MSL8-YFP*

291   in the *msl8-4* background strongly suppressed pollen germination, while the overexpression of *MSL8^{F720L}*-

292   *YFP* did not. The germination rate of *msl8-4* pollen was partially suppressed by expressing

293   *LAT52pMSL8^{I711S}-YFP*, with the strongest-expressing line, I711S-4, germinating 22% of the time and

294   I711S-7 and I711S-12 germinating at rates comparable to L*er*. This indicates that overexpression of

295   MSL8^{F720L} does not rescue the elevated germination and bursting rate of *msl8-4* pollen, and

296   overexpression of MSL8^{I711S} produces a partial reduction in both bursting and germination rates.

297

298   We previously observed that overexpressing *MSL8* reduces pollen fertility, likely through the suppression

299   of germination (Hamilton et al., 2015a). This fertility defect can be observed as a reduction in the

300   transmission of the transgene from the hemizygous T1 generation to the segregating T2 generation, as

301   determined by resistance to the herbicide Basta, which is conferred by the transgene. As expected, three

302   lines expressing *LAT52pMSL8-YFP* in the *msl8-4* background exhibited a significant reduction in

303   transgene transmission, reducing Basta resistance from the expected 75% to around 65%. However,

304   none of the lines overexpressing *MSL8^{I711S}-YFP* or *MSL8^{F720L}-YFP* in the *msl8-4* background showed a

305   significant deviation from the expected rate of resistance (Table 2). This indicates that neither MSL8^{I711S}

306   nor MSL8^{F720L} have an effect on pollen fertility and suggests that the partial suppression of *in vitro*

307   germination conferred by overexpressing *MSL8^{I711S}-YFP* in the *msl8-4* background is insufficient to

308   reduce pollen fertility *in vivo*. Thus, while neither MSL8^{F720L} nor MSL8^{I711S} provide clear function in pollen

309   when expressed at endogenous levels, MSL8^{I711S} can provide some function when expressed at high

310   levels.

311

312   *Overexpressing MSL8^{F720L} in wild-type pollen increases bursting, while overexpressing MSL8 and*

313   *MSL8^{I711S} suppresses pollen germination.*

314   We also investigated the function of MSL8^{I711S} and MSL8^{F720L} when overexpressed in the wild type

315   background, rather than in the *msl8-4* background as above. Transgenic *LAT52pMSL8-YFP,*

316   *LAT52pMSL8^{F720L}-YFP*, or *LAT52pMSL8^{I711S}-YFP* lines were selected wherein *MSL8* or *MSL8* variants

317   were expressed at levels similar to or higher than the endogenous *MSL8* gene (Fig. 8A). Quantitative

318   RT-PCR revealed that transcript levels of endogenous *MSL8* were not significantly different from L*er* in

319   the transgenic lines (Fig. 8A, dark gray bars), while total *MSL8* transcripts were increased over

320   endogenous levels between 1.3 and 4.3-fold (Fig. 8A, light gray bars).

321

322   Pollen from lines expressing *LAT52pMSL8-YFP* and *LAT52pMSL8^{I711S}-YFP* did not germinate at all after

323   incubation in germination media for 6 hours, and the bursting rate of ungerminated pollen grains was

324   reduced to less than 7% (Fig. 8B). The pattern of pollen germination and bursting was indistinguishable

325   between line WT-10 and the three lines overexpressing *MSL8^{I711S}-YFP* as determined by a chi-squared

326   test (Fig. 8B, Supplementary Table S3). However, L*er* pollen expressing *LAT52pMSL8^{F720L}-YFP* burst

327   46% to 54% of the time, comparable to the bursting rate of *msl8-4*. Thus, overexpressing *MSL8^{F720L}* in the

328   wild-type background produced a dominant negative effect, phenocopying the *msl8-4* mutant bursting

329   rate. This elevated bursting rate is likely caused by MSL8^{F720L} disrupting the native pool of MSL8 through

330   the formation of heteromeric channels (see discussion).

331

332   When incubated in germination media overnight, pollen overexpressing MSL8^{F720L} in the L*er* background

333   germinated at rates between that of L*er* and *msl8-4*, indicating that it had little, if any, effect (Fig. 8C).

334   However, overexpressing MSL8^{I711S} in the wild type background resulted in a partial suppression of

335   germination rates, to between 9% and 18%. While line I711S-2 had a germination rate that was

336   indistinguishable from the pollen overexpressing wild type MSL8, the other two independent lines

337   produced pollen germination rates that were both significantly lower than that of L*er* and significantly

338   higher than L*er* + *LAT52pMSL8-YFP* lines, representing an intermediate phenotype.

339

340   We also quantified the effect of *MSL8* overexpression on male fertility in these lines via the segregation of

341   resistance to Basta. Overexpressing *LAT52pMSL8-YFP* in the L*er* background reduced Basta resistance

342   in the segregating T2 generation from 75% to less than 65% (Table 3). One line expressing

343   *LAT52pMSL8^{I711S}-YFP* also exhibited a significant reduction in Basta resistance, to 59%, but all other

344   MSL8 variant lines did not. This indicates that MSL8^{F720L} overexpression does not have an effect on

345   pollen fertility, and suggests that the partial suppression of *in vitro* pollen germination produced by

346   overexpressing   *MSL8^{I711S}*   has   only   a   modest   effect   *in   vivo.*

347

348   **Discussion**

349   *Tension-sensitive ion transport activity of MSL8 is critical for its function in pollen.*

350   A role for MS ion channels in the response of pollen to mechanical and osmotic challenges was

351   proposed more than 20 years ago (Feijo et al., 1995). Such a role has been solidly established for the

352   canonical MS ion channel from *E. coli*, MscS (Edwards et al., 2005; Levin and Blount, 2004; Levina et al.,

353   1999; Miller, 2003; Sukharev et al., 1994), and an initial analysis suggested that of a MscS homolog from

354   Arabidopsis, MSL8, might as well (Hamilton et al., 2015a). However, it remained possible that MSL8

355   could play an indirect role in pollen, perhaps signaling independently of ion flux like close homolog MSL10

356   (Veley et al., 2014). Here we used site-directed mutagenesis, electrophysiology, and physiological assays

357   to determine if the critical function of the MS ion channel MSL8 during pollen hydration and germination is

358   to mediate ion flux.

359

360   *Mutating conserved hydrophobic residues in the pore-lining domain of MSL8 resulted in diminished or*

361   *disrupted channel function.*

362   We identified two point mutations that, when introduced into the presumptive pore-lining helix, altered

363   MSL8 channel behavior without appreciably altering expression, stability, or subcellular localization (Figs.

364   1, 2, Table 1). When expressed in *Xenopus* oocytes, MSL8^{I711S} produced MS currents with a unitary

365   conductance identical to that produced by MSL8 (at pipette potentials from 0-80 mV, 60.7 and. 60.0 pS

366   respectively). However, approximately twice the suction (-29.5 ± 11.7 mmHg for MSL8^{I711S} compared to -

367   18.0 ± 13.1 mmHg for MSL8) was required to open the first MSL8^{I711S} channel compared to the wild type.

368   Thus, MSL8^{I711S} appears relatively insensitive to membrane tension (requiring greater forces to open).

369   When expressed in oocytes, MSL8^{F720L} did produce MS currents that were never observed in water-

370   injected oocytes. However, these MS currents did not form the step-wise increase in current characteristic

371   of individual channel gating events, instead appearing as a flickering increase in current that disappeared

372   immediately after suction was released. Producing these MS currents required higher negative pressures

373   than was required for either MSL8 or MSL8^{I711S}. From this we conclude that MSL8^{F720L} is still able to

374 conduct ions through its pore, but is unable to form a stable open state or to transition normally between

375 non-conducting and conducting configurations.

376

377 *Disrupting normal channel function prevents MSL8 from complementing known msl8-4 loss-of-*

378 *function phenotypes.*

379 Our finding that the severely disrupted MSL8^{F720L} channel was unable to rescue *msl8-4* loss-of-function

380 phenotypes either at native levels of expression (Figs. 2-4) or when overexpressed (Figs. 5-7)

381 demonstrated that a functional channel is necessary for MSL8 to protect pollen from the osmotic stress it

382 experiences during hydration and germination. This supports a model where MSL8 functions akin to

383 MscS, acting as an osmotic pressure release valve (Booth and Blount, 2012), albeit during

384 developmentally programmed osmotic challenges rather than in response to environmental swings in

385 osmolarity. During pollen germination and tube growth, which are powered by internal turgor pressure

386 (Benkert et al., 1997; Zerzour et al., 2009), pollen must have multiple mechanisms to ensure that internal

387 pressure and growth rates do not overtake the delivery of cell wall materials to the growing tip or the

388 strength of the cell wall itself (Hill et al., 2012; Kroeger et al., 2011; Zerzour et al., 2009); MSL8 appears

389 to be one of those mechanisms.

390

391 *Increasing the tension threshold of the MSL8 channel reduces its physiological activity in pollen.*

392 The Ile711Ser mutation increased the force required to gate MSL8, but left wild-type conductance intact–

393 and reduced the ability of MSL8^{I711S} to complement mutant phenotypes. Only when overexpressed could

394 MSL8^{I711S} protect pollen from the hypoosmotic shock of rehydration and maintain the integrity of the

395 pollen tube. Likewise, MSL8^{I711S} only suppressed pollen germination when overexpressed, and not as

396 strongly as the wild type. (Figs. 6-8). These results suggest that wild-type tension sensitivity is crucial for

397 the proper function of MSL8 in pollen. Protection against the hypoosmotic stress of rehydration,

398 maintenance of pollen tube integrity against bursting, and the negative regulation of pollen germination all

399 appear to require that MSL8 gate at tensions below those that open MSL8^{I711S} under native levels of

400 expression.

401

402 Although the evidence described above is consistent with MSL8 functioning like an osmotic safety valve,

403 we note that we cannot exclude the possibility that the ion flow across MSL8 could act as a biochemical

404 signal that indirectly achieves the same function.

405 One example of such biochemical signaling in pollen is the tip-focused Ca^{2+} gradient that regulates pollen

406 tube elongation. High concentrations of Ca^{2+} at the growing pollen tube tip are essential for pollen tube

407 growth (Miller et al., 1992) and require the cyclic nucleotide-gated channel CNGC18 (Gao et al., 2016).

408 Ca^{2+} acts as a crucial secondary messenger in several pathways in order to properly regulate pollen tube

409 growth and guidance to the female gametophyte (Guan et al., 2013). It remains formally possible, though

410 unlikely, that the Ile711Ser or Phe720Leu mutations affect both the characteristics of the channel and the

411 function of other domains important for signaling independent of ion transport. Lesions in both the soluble

412 N-terminus (Veley et al., 2014) and the soluble C-terminus (Zou et al., 2015) affect the cell death

413 signaling function of MSL10, but lesions to the predicted pore-lining domain have not yet been tested.

414 Future work will be required to understand how MSL8 functions alongside established ion channels and

415 the tightly regulated ion fluxes that are essential for pollen germination and tube growth (Michard et al.,

416 2009).

417

418 *MSL8[F720L] has reduced channel activity and can act as a dominant negative allele.*

419 The substitution of Leu for Phe at positon 720 in MSL8 both increased the threshold required to produce

420 MS currents and prevented the appearance of the step-wise increases in current that are indicative of a

421 discrete transition from closed to open configurations, suggesting instability in the channel (Fig. 1B,

422 bottom left panel, Supplementary Fig. S1, Table 1). The closed form of *Ec*MscS is proposed to involve

423 close packing of small residues from adjoining pore-lining domains (Edwards et al., 2005). The

424 substitution of large hydrophobic residues for Gly or Ala at these positions results in less stable open

425 state configurations with higher tension thresholds, that at least superficially resemble MSL8[F720L]

426 (Edwards et al., 2005; Rasmussen et al., 2015; Wu et al., 2011). Alternating chains of small hydrophobic

427 amino acids are not observed in the predicted pore-lining domain of MSL8 (Fig. 1B). Rather, a repeating

428 pattern of large hydrophobic/polar residues in the predicted pore-lining domain is conserved among the

429 seven Arabidopsis MscS homologs predicted to localize to the plasma membrane. These residues

430   include three phenylalanines at positions 710, 720 and 727 (marked with arrowheads, Supplementary

431   Fig. S3). The observed channel characteristics of MSL8[F720L] suggest that the pairing of similarly sized

432   residues in the pore-lining domains may be an important factor in maintaining the stability and normal

433   function of both MscS and MSLs. Testing this idea will require additional study, in particular detailed

434   structural information for the plasma membrane-localized MSLs.

435

436   Expressing *MSL8[F720L]* in a wild type background, and therefore in the presence of a native pool of MSL8,

437   phenocopies the mutant with respect to germination rate and pollen tube bursting (Fig. 8B-C). Because

438   MSLs are likely to form homomeric channels (Haswell et al., 2008; Peyronnet et al., 2008), this dominant

439   negative effect is likely caused by the formation of heteromeric channel complexes. According to this

440   model, the instability caused by the Phe720Leu mutation is dominantly imparted to MSL8-MSL8[F720L]

441   heteromeric channels, reducing the number of functional MSL8 channels available, and thereby

442   producing pollen with characteristics similar to those from the loss-of-function *msl8-4* background. A

443   similar effect was described for the *Caenorhabditis elegans* TRP-4 candidate MS ion channel (Kang et

444   al., 2010). A TRP-4 mutant that did not form a functional channel on its own dominantly ablated channel

445   function when co-expressed with wild type TRP-4 in touch-sensitive neurons. How many MSL8[F720L]

446   monomers are sufficient to disrupt the function of an otherwise wild type MSL8 channel is not yet known.

447

448   *MSL8[I711S] can complement the msl8-4 mutant only when overexpressed, consistent with a cooperative*

449   *gating mechanism.*

450   MSL8[I711S] exhibited both an elevated tension threshold and reduced function *in planta*. MSL8 Ile711

451   aligns with Ala110 of *Ec*MscS (Fig. 1B), and a mutation in the neighboring residue, Leu111, produces a

452   similar disruption in function. In *Ec*MscS, Leu111Ser is associated with a doubled tension threshold, and

453   MscSL[111S] is unable to protect *E. coli* against osmotic shock (Belyy et al., 2010). Leu111 is part of the

454   proposed "tension-transmitting clutch" that allows *Ec*MscS to respond to increases in membrane tension

455   through hydrophobic associations with the other TM helices. The substitution of a hydrophilic residue for a

456   hydrophobic one may weaken these interactions. Our data presented here show that Ile711 may play a

457   similar force-transmitting role in MSL8. Once open, MSL8[I711S] appears to produce a normal pore, as its

458   single-channel conductance was wild type.

459

460   There are several possible explanations for the ability of MSL8[I711S] to partially rescue loss-of-function

461   phenotypes at high levels of expression. First, the gating of a MS ion channel is a stochastic process

462   centered on the average tension threshold (Hille, 1992). Increasing the population of MSL8[I711S] channels

463   in pollen would increase the number of channels available in the population to open at lower tensions,

464   potentially to levels sufficient for protection against osmotic stress. We do not favor this model, primarily

465   because we do not see a linear increase in complementation associated with expression level. Instead,

466   when expressed at endogenous levels MSL8[I711S] is completely unable to rescue mutant phenotypes.

467

468   Alternatively, MSL8 could participate in cooperative gating. Cooperative gating is the lowering of the

469   average tension threshold as the number of channels embedded in the membrane increases. Biophysical

470   modeling experiments with *Ec*MscL have shown that local deformation of the lipid bilayer at the channel

471   periphery could explain the energetics of cooperative gating (Haselwandter and Phillips, 2013; Ursell et

472   al., 2007). If MSL8[I711S] is expressed at high enough levels, cooperative gating might reduce the tension

473   threshold enough to allow it to protect pollen during hydration.

474

475   Cooperative gating could also explain the observation that overexpressing wild-type MSL8 in the L*er*

476   background suppresses pollen germination (Fig. 8B, (Hamilton et al., 2015a)). It is thought that high

477   turgor pressure is required for breaking through the cell wall during germination (Feijo et al., 1995). If

478   overexpression results in MSL8 channel activity at lower membrane tensions by promoting cooperative

479   gating, then the critical turgor for germination might never be reached. Pollen would then be stuck in a

480   futile cycle of building pressure, relieving pressure, and building it again. In support of this idea, we

481   observed that pollen overexpressing MSL8 developed the larger and more structured vacuole

482   morphology resembling normally germinating pollen (Supplementary Fig. S4; (Hicks et al., 2004; Wudick

483   et al., 2014)), though it rarely went on to germinate. Future work will determine if MSL8 and MSL8[I711S]

484   exhibit cooperative gating in *Xenopus* oocytes.

485

486   *MSL8 fulfills all criteria for assignment as a mechanotransducer.*

487   The four criteria necessary for establishing a protein as the transducer of a physiological mechanical

488   response are: (1) it is expressed in the correct cell and subcellular location to respond to mechanical

489   stimulation; (2) it is required for the mechanosensory response, not the normal development of the cell;

490   (3) it forms a MS channel in a heterologous system; and (4) structural changes that affect the protein's

491   response in a heterologous system affect its function *in vivo* (Arnadottir and Chalfie, 2010). MscL and

492   MscS in bacteria fulfill these criteria (Edwards et al., 2005; Levin and Blount, 2004; Levina et al., 1999;

493   Miller, 2003; Sukharev et al., 1994), and NOMPC of *Drosophila* was recently shown to be a

494   mechanotransducer of touch response in touch-sensitive neurons (Gong et al., 2013; Yan et al., 2013).

495

496   MSL8 now fulfills all four criteria: (1) it is expressed in tricellular and mature pollen and pollen tubes, and

497   localizes to the plasma membrane; (2) it is not required for the normal development of pollen, but is

498   required for protection against osmotic stress; (3) it forms a MS channel in the heterologous *Xenopus*

499   oocyte system; and (4) altering its structure changes its electrophysiological characteristics and its

500   physiological function, without affecting expression or subcellular localization.

501

502   Pollen faces additional, relatively unstudied mechanical challenges during its development, and

503   mechanically sensitive proteins are likely to be involved. Desiccation is critical for the success of pollen

504   from most species (Franchi et al., 2011), and presents unique osmotic and mechanical challenges (Firon

505   et al., 2012; Hoekstra et al., 1997; 2001). Furthermore, as it invades the sporophytic tissue to reach the

506   female gametophyte, the pollen tube must sense, produce, and regulate the forces required to grow in

507   between other cells (Sanati Nezhad et al., 2013). Finally, the regulated process of bursting that must

508   occur to release the sperm cells from within the pollen tube represents a fascinating case where

509   mechanisms that previously maintained the structural integrity of the cell must be overcome in order to

510   complete fertilization (Amien et al., 2010; Dresselhaus et al., 2016; Woriedh et al., 2013). Using

511   electrophysiology, mutagenesis and physiological assays, we discovered that mechanosensitive ion

512   channels are one mechanism pollen relies on to respond to the mechanical effects of osmotic changes.

513   This powerful combination of techniques, as well as the development of new tools to probe pollen in the

514   dry state, may uncover other mechanical and ionic regulation strategies in pollen and other plant cells.

515

516 **Materials and Methods**

517

518 *Plant material and growth conditions.* Plants were grown on soil under 24 hours of light at 21°C. *msl8-4*

519 (DsLoxN101568 and DsLoxN101751, in the L*er* background) was obtained from the Arabidopsis

520 Biological Resource Center. MSL8^{I711S} and MSL8^{F720L} constructs were produced through site-directed

521 mutagenesis from existing vectors (described in (Hamilton et al., 2015)) and transformed into *msl8-4* or L-

522 *er* by floral dip.

523

524 *Multiple alignments.* Alignments were performed in MEGA7 using a Clustal alignment with a pairwise

525 alignment gap opening penalty of 10 and gap extension penalty of 0.1 and a multiple alignment gap

526 opening penalty of 10 and gap extension penalty of 0.2. Sequences for alignment were based on

527 previous phylogenetic analysis of *Ec*MscS and Arabidopsis MSLs (Haswell, 2007) predicting the pore-

528 lining domains of MSLs based on the known pore-lining domain of *Ec*MscS.

529

530 *Electrophysiology.* Single channel patch-clamp electrophysiology was performed as described in

531 (Maksaev and Haswell, 2015). Capped RNA (cRNA) of *MSL8* was transcribed *in vitro* using the

532 mMESSAGE mMACHINE SP6 kit (Ambion) and stored at 1µg/µl at -80 °C. Defolliculated oocytes were

533 purchased from Xenopus1 (Dexter, MI) and injected with 50 nl of cRNA or water and patched in

534 symmetric 60 mM MgCl$_2$ after incubating for 2-10 days in ND96 buffer + gentamycin.

535

536 *Reverse-transcriptase-polymerase chain reaction.* RNA was isolated from floral tissue (stage 13/14

537 flowers) using the Qiagen RNeasy Mini RNA extraction kit (Qiagen). cDNA was generated from 2 µg RNA

538 using an oligo(dT)$_{20}$ primer and the M-MLV Reverse Transcriptase kit (Promega). *ACTIN,* total *MSL8,*

539 endogenous *MSL8* and *MSL8-YFP* transcripts were amplified with the primers listed in Supplementary

540 Table S4 using SYBR Green PCR Master Mix (Applied Biosciences) and 0.25 µL cDNA at a final volume

541 of 25 µL. Quantitative RT-PCR was performed using the StepOnePlus real-time PCR system (Applied

542 Biosystems). Total *MSL8* was amplified using primers that do not distinguish between the endogenous

543   locus and the transgenes. Endogenous *MSL8* was amplified using a reverse primer in the 3' UTR, which

544   is not present in the transgenes.

545

546   *In vitro pollen hydration.* Pollen from mature (stage 13-14) flowers was hydrated in 25-30 µl drops of

547   water or the indicated percentage of PEG (average molecular weight 3350 g/mol, Sigma-Aldrich) at a final

548   concentration of 1 µg/ml fluorescein diacetate (FDA, Sigma-Aldrich) and 0.5 µg/ml propidium iodide (PI,

549   Sigma-Aldrich) on double-ring cytology slides. Slides were inverted and incubated in a humid chamber at

550   room temperature for the indicated amount of time. To image, cover slips were added and FDA signal

551   was collected in the GFP epifluorescence channel while PI signal was collected in the dsRed

552   epifluorescence channel. FDA stains live pollen while PI enters dead pollen.

553

554   *In vitro pollen germination.* Pollen germination was performed according to (Daher, Chebli, Geitmann

555   2009 Plant Cell Rep). Pollen was pre-hydrated by removing flowers from plants and incubating for 45

556   minutes at 30°C in a humid chamber constructed from a large petri dish containing smaller petri dishes

557   placed on top of moistened filter paper. Pollen was incubated in 30 µl of pollen germination media (2 mM

558     $CaCl_2$, 2 mM $Ca(NO_3)_2$, 0.49 mM H_3BO_3, 1 mM $MgSO_4$, 1 mM KCl, 18% w/v sucrose, pH 7) at 30°C for 6

559   or 16 hours in a humid chamber as during pollen hydration. Pollen was counted as germinated if it had

560   produced a pollen tube longer than the pollen grain. Pollen was counted as burst if expelled cytoplasm

561   was visible outside the pollen grain or pollen tube.

562

563   *Microscopy.* Confocal images of GFP or YFP signal in pollen were acquired on an Olympus BX-61

564   microscope using FV10-ASW Olympus software and the GFP (488 nm excitation, 505-605 nm bandpass

565   filter) or YFP (515 nm excitation, 535-565 nm bandpass filter) channels. Brightfield and epifluorescent

566   images for pollen germination and pollen viability assays were collected on the same microscope using

567   an Olympus DP71 digital camera, DP Controller software, and filter sets for GFP (470/40 nm excitation,

568   525/50 nm emission) or dsRED (545/30 nm excitation, 620/60 nm emission).

569

570 *Calculation of transmission ratios.* The transmission frequencies of the *MSL8* transgenes were

571 determined by selecting seedlings from the T2 generation with Basta on soil and counting the number of

572 sensitive and resistant progeny. The Basta resistance gene *bar* is included in the transgene.

573

574 *Statistical analyses.* One-way or two-way ANOVAs were performed as indicated in figure legends.

575 Tukey's HSD post-hoc test was used to determine statistical significance for balanced data sets.

576 Scheffe's post-hoc test was used to determine statistical significance for unbalanced data sets. Chi-

577 squared tests with Bonferroni correction were performed for analysis of transgene transmission and for

578 comparison between groups of the pattern of germinated and burst pollen during pollen germination

579 assays.

580

581 **Funding**

584

585 **Disclosures**

586 The authors have no conflicts of interest to declare.

587

588 **Acknowledgements**

591

592 **References**

593 Amien, S., Kliwer, I., Márton, M.L., Debener, T., Geiger, D., Becker, D., et al. (2010). Defensin-like
594 ZmES4 mediates pollen tube burst in maize via opening of the potassium channel KZM1. PLoS Biology *8*,
595 e1000388.

596 Anishkin, A., and Sukharev, S. (2004). Water Dynamics and Dewetting Transitions in the Small
597 Mechanosensitive Channel MscS. Biophysical Journal *86*, 2883–2895.

598 Arnadottir, J., and Chalfie, M. (2010). Eukaryotic mechanosensitive channels. Annual Review of
599 Biophysics *39*, 111–137.

Bass, R.B., Strop, P., Barclay, M., and Rees, D.C. (2002). Crystal structure of Escherichia coli MscS, a voltage-modulated and mechanosensitive channel. Science *298*, 1582–1587.

Beauzamy, L., Nakayama, N., and Boudaoud, A. (2014). Flowers under pressure: ins and outs of turgor regulation in development. Annals of Botany *114*, 1517–1533.

Belyy, V., Anishkin, A., Kamaraju, K., Liu, N., and Sukharev, S. (2010). The tension-transmitting "clutch" in the mechanosensitive channel MscS. Nat Struct Mol Biol *17*, 451–458.

Benkert, R., Obermeyer, G., and Bentrup, F.-W. (1997). The turgor pressure of growing lily pollen tubes. Protoplasma *198*, 1–8.

Booth, I.R., and Blount, P. (2012). The MscS and MscL families of mechanosensitive channels act as microbial emergency release valves. J. Bacteriol. *194*, 4802–4809.

Burg, M.B., and Ferraris, J.D. (2008). Intracellular organic osmolytes: function and regulation. J. Biol. Chem. *283*, 7309–7313.

Chen, L.-Y., Shi, D.-Q., Zhang, W.-J., Tang, Z.-S., Liu, J., and Yang, W.-C. (2015). The Arabidopsis alkaline ceramidase TOD1 is a key turgor pressure regulator in plant cells. Nature Communications *6*, 6030.

Dresselhaus, T., and Franklin-Tong, N. (2013). Male-female crosstalk during pollen germination, tube growth and guidance, and double fertilization. Molecular Plant *6*, 1018–1036.

Dresselhaus, T., Sprunck, S., and Wessel, G.M. (2016). Fertilization Mechanisms in Flowering Plants. Current Biology *26*, R125–R139.

Edlund, A.F. (2004). Pollen and Stigma Structure and Function: The Role of Diversity in Pollination. The Plant Cell *16*, S84–S97.

Edwards, M.D., Li, Y., Kim, S., Miller, S., Bartlett, W., Black, et al. (2005). Pivotal role of the glycine-rich TM3 helix in gating the MscS mechanosensitive channel. Nat Struct Mol Biol *12*, 113–119.

Feijo, J.A., Malh, R., and Obermeyer, G. (1995). Ion dynamics and its possible role during in vitro pollen germination and tube growth. Protoplasma *187*, 155–167.

Firon, N., Nepi, M., and Pacini, E. (2012). Water status and associated processes mark critical stages in pollen development and functioning. Annals of Botany *109*, 1201–1214.

Franchi, G.G., Piotto, B., Nepi, M., Baskin, C.C., Baskin, J.M., and Pacini, E. (2011). Pollen and seed desiccation tolerance in relation to degree of developmental arrest, dispersal, and survival. Exbotj *62*, 5267–5281.

Gao, Q.-F., Gu, L.-L., Wang, H.-Q., Fei, C.-F., Fang, X., Hussain, J., et al. (2016). Cyclic nucleotide-gated channel 18 is an essential Ca 2+channel in pollen tube tips for pollen tube guidance to ovules in Arabidopsis. Proc Natl Acad Sci USA *113*, 3096–3101.

Gong, J., Wang, Q., and Wang, Z. (2013). NOMPC is likely a key component of Drosophilamechanotransduction channels. Eur J Neurosci *38*, 2057–2064.

Guan, Y., Guo, J., Li, H., and Yang, Z. (2013). Signaling in Pollen Tube Growth: Crosstalk, Feedback, and Missing Links. Molecular Plant *6*, 1053–1064.

Hafidh, S., Fíla, J., and Honys, D. (2016). Male gametophyte development and function in angiosperms: a

638   general concept. Plant Reproduction 1–21.

639   Hamilton, E.S., Jensen, G.S., Maksaev, G., Katims, A., Sherp, A., and Haswell, E.S. (2015a).
640   Mechanosensitive channel MSL8 regulates osmotic forces during pollen hydration and germination.
641   Science *350*, 438–441.

642   Hamilton, E.S., Schlegel, A.M., and Haswell, E.S. (2015b). United in Diversity: Mechanosensitive Ion
643   Channels in Plants. Annu. Rev. Plant Biol.

644   Haselwandter, C.A., and Phillips, R. (2013). Directional interactions and cooperativity between
645   mechanosensitive membrane proteins. Europhys Lett *101*, 68002p1–68002p6.

646   Haswell, E.S. (2007). MscS☐Like Proteins in Plants. *58*, 329–359.

647   Haswell, E.S., and Meyerowitz, E.M. (2006). MscS-like Proteins Control Plastid Size and Shape in
648   Arabidopsis thaliana. Current Biology *16*, 1–11.

649   Haswell, E.S., Peyronnet, R., Barbier-Brygoo, H., Meyerowitz, E.M., and Frachisse, J.-M. (2008). Two
650   MscS Homologs Provide Mechanosensitive Channel Activities in the Arabidopsis Root. Current Biology
651   *18*, 730–734.

652   Hicks, G.R., Rojo, E., Hong, S., Carter, D.G., and Raikhel, N.V. (2004). Geminating pollen has tubular
653   vacuoles, displays highly dynamic vacuole biogenesis, and requires VACUOLESS1 for proper function.
654   Plant Physiology *134*, 1227–1239.

655   Hill, A.E., Shachar-Hill, B., Skepper, J.N., Powell, J., and Shachar-Hill, Y. (2012). An Osmotic Model of
656   the Growing Pollen Tube. PLoS ONE *7*, e36585.

657   Hille, B. (1992). Ionic Channels of Excitable Membranes (Sunderland, Massachusetts: Sinauer
658   Associates Incorporated).

659   Hoekstra, F.A., Golovina, E.A., and Buitink, J. (2001). Mechanisms of plant desiccation tolerance. Trends
660   in Plant Science *6*, 431–438.

661   Hoekstra, F.A., Wolkers, W.F., Buitink, J., Golovina, E.A., Crowe, J.H., and Crowe, L.M. (1997).
662   Membrane Stabilization in the Dry State. Comparative Biochemistry and Physiology Part a: Physiology
663   *117*, 335–341.

664   Jeffries, K.M., Hinch, S.G., Donaldson, M.R., Gale, M.K., Burt, J.M., Thompson, L.A., Farrell, A.P., et al.
665   (2011). Temporal changes in blood variables during final maturation and senescence in male sockeye
666   salmon Oncorhynchus nerka: reduced osmoregulatory ability can predict mortality. J. Fish Biol. *79*, 449–
667   465.

668   Kang, L., Gao, J., Schafer, W.R., Xie, Z., and Xu, X.Z.S. (2010). C. elegans TRP Family Protein TRP-4 Is
669   a Pore-Forming Subunit of a Native Mechanotransduction Channel. Neuron *67*, 381–391.

670   Kloda, A., and Martinac, B. (2002). Common evolutionary origins of mechanosensitive ion channels in
671   Archaea, Bacteria and cell-walled Eukarya. Archaea *1*, 35–44.

672   Koprowski, P., and Kubalski, A. (2003). C Termini of the Escherichia coli Mechanosensitive Ion Channel
673   (MscS) Move Apart upon the Channel Opening. J. Biol. Chem. *278*, 11237–11245.

674   Kroeger, J.H., Zerzour, R., and Geitmann, A. (2011). Regulator or Driving Force? The Role of Turgor
675   Pressure in Oscillatory Plant Cell Growth. PLoS ONE *6*, e18549.

676 Kung, C., Martinac, B., and Sukharev, S. (2010). Mechanosensitive channels in microbes. Annu. Rev.
677 Microbiol. *64*, 313–329.

678 Labarca, C., Kroh, M., and Loewus, F. (1970). The Composition of Stigmatic Exudate from Lilium
679 longiflorum: Labeling Studies with Myo-inositol, D-Glucose, and L-Proline. Plant Physiology *46*, 150–156.

680 Lai, J.Y., Poon, Y.S., Kaiser, J.T., and Rees, D.C. (2013). Open and shut: Crystal structures of the
681 dodecylmaltoside solubilized mechanosensitive channel of small conductance from Escherichia coliand
682 Helicobacter pyloriat 4.4 Å and 4.1 Å resolutions. Protein Science *22*, 502–509.

683 Lee, C.P., Maksaev, G., Jensen, G.S., Murcha, M.W., Wilson, M.E., Fricker, M., et al. (2016). MSL1 is a
684 mechanosensitive ion channel that dissipates mitochondrial membrane potential and maintains redox
685 homeostasis in mitochondria during abiotic stress. Plant J.

686 Levin, G., and Blount, P. (2004). Cysteine Scanning of MscL Transmembrane Domains Reveals
687 Residues Critical for Mechanosensitive Channel Gating. Biophysical Journal *86*, 2862–2870.

688 Levina, N., Tötemeyer, S., Stokes, N.R., Louis, P., Jones, M.A., and Booth, I.R. (1999). Protection of
689 Escherichia coli cells against extreme turgor by activation of MscS and MscL mechanosensitive channels:
690 identification of genes required for MscS activity. The EMBO Journal *18*, 1730–1737.

691 Maksaev, G., and Haswell, E.S. (2015). Expressing and characterizing mechanosensitive channels in
692 Xenopus oocytes. Methods in Molecular Biology *1309*, 151–169.

693 Maksaev, G., and Haswell, E.S. (2012). MscS-Like10 is a stretch-activated ion channel from Arabidopsis
694 thaliana with a preference for anions. Proc Natl Acad Sci USA *109*, 19015–19020.

695 Malcolm, H.R., and Maurer, J.A. (2012). The Mechanosensitive Channel of Small Conductance (MscS)
696 Superfamily: Not Just Mechanosensitive Channels Anymore. ChemBioChem *13*, 2037–2043.

697 Michard, E., Alves, F., and Feijo, J.A. (2009). The role of ion fluxes in polarized cell growth and
698 morphogenesis: the pollen tube as an experimental paradigm. Int. J. Dev. Biol. *53*, 1609–1622.

699 Miller, D.D., Callaham, D.A., Gross, D.J., and Hepler, P.K. (1992). Free Ca2+ gradient in grow pollen
700 tubes of Lilium. Journal of Cell Science 7–12.

701 Miller, S. (2003). Domain organization of the MscS mechanosensitive channel of Escherichia coli. The
702 EMBO Journal *22*, 36–46.

703 Pacini, E., Guarnieri, M., and Nepi, M. (2006). Pollen carbohydrates and water content during
704 development, presentation, and dispersal: a short review. Protoplasma *228*, 73–77.

705 Peyronnet, R., Haswell, E.S., Barbier-Brygoo, H., and Frachisse, J.-M. (2008). AtMSL9 and AtMSL10:
706 Sensors of plasma membrane tension in Arabidopsis roots. Plant Signaling & Behavior *3*, 726–729.

707 Pivetti, C.D., Yen, M.R., Miller, S., Busch, W., Tseng, Y.H., Booth, I.R., et al. (2003). Two Families of
708 Mechanosensitive Channel Proteins. Microbiology and Molecular Biology Reviews *67*, 66–85.

709 Porter, B.W., Zhu, Y.J., Webb, D.T., and Christopher, D.A. (2009). Novel thigmomorphogenetic
710 responses in Carica papaya: touch decreases anthocyanin levels and stimulates petiole cork outgrowths.
711 Annals of Botany *103*, 847–858.

712 Prole, D.L., and Taylor, C.W. (2013). Identification and Analysis of Putative Homologues of
713 Mechanosensitive Channels in Pathogenic Protozoa. PLoS ONE *8*, e66068–e66069.

714   Ranade, S.S., Syeda, R., and Patapoutian, A. (2015). Mechanically Activated Ion Channels. Neuron *87*,
715   1162–1179.

716   Rasmussen, T., Rasmussen, A., Singh, S., Galbiati, H., Edwards, M.D., Miller, S., et al. (2015). Properties
717   of the Mechanosensitive Channel MscS Pore Revealed by Tryptophan Scanning Mutagenesis.
718   Biochemistry *54*, 4519–4530.

719   Samuel, M.A., Chong, Y.T., Haasen, K.E., Aldea-Brydges, M.G., Stone, S.L., and Goring, D.R. (2009).
720   Cellular pathways regulating responses to compatible and self-incompatible pollen in Brassica and
721   Arabidopsis stigmas intersect at Exo70A1, a putative component of the exocyst complex. The Plant Cell
722   *21*, 2655–2671.

723   Sanati Nezhad, A., Naghavi, M., Packirisamy, M., Bhat, R., and Geitmann, A. (2013). Quantification of
724   cellular penetrative forces using lab-on-a-chip technology and finite element modeling. Proceedings of the
725   National Academy of Sciences of the United States of America *110*, 8093–8098.

726   Steinbacher, S., Bass, R., Strop, P., and Rees, D.C. (2007). Structures of the Prokaryotic
727   Mechanosensitive Channels MscL and MscS. In Mechanosensitive Ion Channels, Part A, (Elsevier), pp.
728   1–24.

729   Sukharev, S.I., Blount, P., Martinac, B., Blattner, F.R., and Kung, C. (1994). A large-conductance
730   mechanosensitive channel in E. coli encoded by mscL alone. Nature *368*, 265–268.

731   Tovar-Rojo, F., Cabrera-Martinez, R.-M., Setlow, B., and Setlow, P. (2003). Studies on the mechanism of
732   the osmoresistance of spores of Bacillus subtilis. J. Appl. Microbiol. *95*, 167–179.

733   Ursell, T., Huang, K.C., Peterson, E., and Phillips, R. (2007). Cooperative gating and spatial organization
734   of membrane proteins through elastic interactions. PLoS Comput Biol *3*, e81.

735   van Bilsen, D., Hoekstra, F.A., Crowe, L.M., and Crowe, J.H. (1994). Altered Phase Behavior in
736   Membranes of Aging Dry Pollen May Cause Imbibitional Leakage. Plant Physiology *104*, 1193–1199.

737   Veley, K.M., Maksaev, G., Frick, E.M., January, E., Kloepper, S.C., and Haswell, E.S. (2014). Arabidopsis
738   MSL10 has a regulated cell death signaling activity that is separable from its mechanosensitive ion
739   channel activity. The Plant Cell *26*, 3115–3131.

740   Wang, W., Black, S.S., Edwards, M.D., Miller, S., Morrison, E.L., Bartlett, W., Dong, C., et al. (2008). The
741   structure of an open form of an E. coli mechanosensitive channel at 3.45 A resolution. Science *321*,
742   1179–1183.

743   Woriedh, M., Wolf, S., Márton, M.L., Hinze, A., Gahrtz, M., Becker, D., et al. (2013). External application
744   of gametophyte-specific ZmPMEI1 induces pollen tube burst in maize. Plant Reproduction *26*, 255–266.

745   Wu, H.M., Hazak, O., Cheung, A.Y., and Yalovsky, S. (2011). RAC/ROP GTPases and auxin signaling.
746   The Plant Cell *23*, 1208–1218.

747   Wudick, M.M., Luu, D.T., Tournaire-Roux, C., Sakamoto, W., and Maurel, C. (2014). Vegetative and
748   sperm cell-specific aquaporins of Arabidopsis highlight the vacuolar equipment of pollen and contribute to
749   plant reproduction. Plant Physiology *164*, 1697–1706.

750   Yan, Z., Zhang, W., He, Y., Gorczyca, D., Xiang, Y., Cheng, L.E., et al. (2013). Drosophila NOMPC is a
751   mechanotransduction channel subunit for gentle-touch sensation. Nature *493*, 221–225.

752   Zerzour, R., Kroeger, J., and Geitmann, A. (2009). Polar growth in pollen tubes is associated with
753   spatially confined dynamic changes in cell mechanical properties. Developmental Biology *334*, 437–446.

754   Zhang, J. (1999). Genetic analysis of osmotic adjustment in crop plants. Exbotj *50*, 291–302.

755   Zou, Y., Chintamanani, S., He, P., Fukushige, H., Yu, L., Shao, M., et al. (2015). A gain-of-function
756   mutation in Msl10 triggers cell death and wound-induced hyperaccumulation of jasmonic acid in
757   Arabidopsis. Journal of Integrative Plant Biology *58*, 600–609.

758

759

760   **Tables**

761

762   **Table 1. Conductance, tension threshold, and number of observations of MSL8 variants in**

763   ***Xenopus* oocytes**

		Tension Threshold		
	Conductance	First channel to open, mmHg	Last channel to close, mmHg	Patches with activity / total patches
MSL8	60.0	-18.9 ± 13.1	-1.7 ± 3.5	23/26
MSL8[I711S]	60.7	-29.5 ± 11.7	-9.4 ± 9.5	27/32
MSL8[F720L]	NA	-61.2 ± 12.3	-52.7 ± 11.5	20/24
Water	NA	NA	NA	0/26

764

765

766

767

768

769

770
771   **Table 2. Transmission of *LAT52pMSL8-YFP* variant transgenes in the *msl8-4* background**

772

msl8-4 + LAT52pMSL8-YFP	T2 progeny resistant to Basta				
	Line	% Expected	% Observed (number observed/total)	X^2	p
	1	75	67.2 (86/128)	5.18	0.023
MSL8	14	75	66.1 (74/112)	5.79	0.016
	11	75	64.0 (80/125)	9.52	0.002
	1	75	78.3 (47/60)	0.23	0.64
MSL8^{F720L}	10	75	74.4 (29/39)	0.05	0.83
	2	75	75.9 (41/54)	0.01	0.94
	7	75	74.0 (91/12)	0.23	0.64
MSL8^{I711S}	12	75	76.7 (89/116)	0.07	0.79
	4	75	74.1 (86/116)	0.18	0.67

773
774 **Table 3. Transmission of *LAT52pMSL8-YFP* variant transgenes in the wild-type background**

775

| Ler + LAT52pMSL8-YFP | Line | T2 progeny resistant to Basta | | | |
		% Expected	% Observed (number observed/total)	X^2	p
MSL8	10	75	60.0 (30/50)	6.00	0.014
	27	75	63.9 (53/83)	5.50	0.019
MSL8^{F720L}	5	75	78.9 (30/38)	0.32	0.57
	6	75	67.3 (66/98)	3.06	0.080
	9	75	76.9 (40/52)	0.10	0.75
MSL8^{I711S}	1	75	58.6 (34/58)	8.30	0.0040
	2	75	65.6 (40/61	2.89	0.089
	4	75	72.3 (34/47)	0.18	0.67

776
777   **Figure Legends**

778

779   **Figure 1. Mutations in the predicted pore-lining domain alter channel properties of MSL8.** (**A**)

780   Predicted topology of MSL8. N and C mark the amino- and carboxy-terminal ends respectively. Thick line

781   marks the predicted pore-lining domain. Residues mutated in this study are indicated. (**B**) Multiple

782   alignment of the predicted pore-lining transmembrane regions of Arabidopsis MSL8, Arabidopsis MSL10

783   and the known pore-lining domain of *E. coli MscS*. Identical residues conserved in at least half of the

784   sequences are shaded darkly; similar residues conserved at this level are shaded in gray. Residues

785   proposed to form the channel seal in *Ec*MscS are marked with arrowheads. MSL8 residues mutated in

786   this study are marked with an asterisk. (**C**) Representative traces from excised inside-out patches of

787   plasma membrane from *Xenopus laevis* oocytes following injection with the indicated cRNA or water

788   clamped at -40 mV membrane potential. (**D**) The current-voltage relationship of MSL8 (squares, $N = 4$

789   oocytes) and MSL8^{I711S} (triangles, $N = 9$ oocytes) in symmetric 60 mM $MgCl_2$. Dashed line indicates the

790   slope from which the single-channel conductance was measured (see Table 1). Error bars are mean ±

791   SE.

792

793   **Figure 2. Expression and subcellular localization of MSL8-GFP expressed from endogenous**

794   **sequences**. (**A**) Quantitative reverse-transcription polymerase chain reaction amplification of *MSL8*

795   transcripts in L*er*, *msl8-4*, and *gMSL8-GFP* transgenic lines. Levels are presented relative to *ACTIN*.

796   Different letter groups indicate significant ($p < 0.05$) differences between groups as determined by

797   Tukey's post-hoc test following one-way ANOVA. Error bars are mean ± SE of three biological and two

798   technical replicates. (**B**) Confocal images of GFP signal in pollen from stage 13-14 flowers from the

799   indicated lines hydrated in water. Scale bar is 20 μm.

800

801   **Figure 3. MSL8^{I711S}-GFP and MSL8^{F720L}-GFP do not complement the *msl8-4* hydration viability**

802   **defect when expressed from endogenous sequences.** (**A**) Hydration viability time course. Mature,

803   desiccated pollen from *msl8-4* + gMSL8-GFP and variant lines hydrated in distilled water for the indicated

804   periods of time. Viability was determined by staining with fluorescein diacetate (which marks live pollen)

805 and propidium iodide (which enters compromised cells). The average of 3-6 experiments with N = 58 –

806 377 pollen grains per experiment is shown. (**B**) Hydration viability in PEG_{3350} series. The average of 3-9

807 experiments with N = 68-566 pollen grains per experiment is presented. Different letter groups indicate

808 significant (p < 0.05) differences between groups as determined by Scheffe's post-hoc test following two-

809 way ANOVA. Error bars are mean ± SE.

810

811 **Figure 4. MSL8^{I711S}-GFP and MSL8^{F720L}-GFP do not suppress *msl8-4* pollen bursting or germination**

812 **when expressed from endogenous sequences.** Mature, desiccated pollen from the indicated lines

813 were incubated in germination media for 6 hours then examined under the microscope. Each pollen grain

814 scored was placed into one of the four indicated categories. Pollen was counted as germinated if it had

815 produced a pollen tube longer than the pollen grain. Pollen was counted as burst if expelled cytoplasm

816 was visible. Averages from 3-6 experiments with N = 101-236 pollen per experiment are presented. See

817 Supplementary Table 1 for statistical differences between groups. Error bars are mean ± SE.

818

819 **Figure 5. Expression and subcellular localization of MSL8^{I711S}-YFP and MSL8^{F720L}-YFP expressed**

820 **from the *LAT52* promoter in the *msl8-4* background.** (**A**) Quantitative reverse-transcription polymerase

821 chain reaction amplification of *MSL8* transcripts, presented relative to *ACTIN*, in L*er*, *msl8-4*, and *msl8-4*

822 + *LAT52pMSL8-YFP* transgenic lines. Error bars are mean ± SE. (**B**) Confocal images of YFP signal in

823 *msl8-4* pollen or *msl8-4* pollen expressing *LAT52pMSL8-YFP*, *LAT52pMSL8^{I711S}-YFP*, or

824 *LAT52pMSL8^{F720L}-YFP*. Scale bars are 20 μm.

825

826 **Figure 6. MSL8^{I711S}-YFP but not MSL8^{F720L}-YFP partially rescues the *msl8-4* hydration viability**

827 **defect when overexpressed in the *msl8-4* background.** Hydration viability time course, performed as

828 described in Fig. 3. The average of 3 to 4 experiments with N = 124 to 354 pollen per experiment is

829 presented. Different letter groups indicate significant (p < 0.05) differences between groups as

830 determined by Scheffe's post-hoc test following two-way ANOVA. Error bars are mean ± SE.

831

832 **Figure 7. MSL8^{I711S}-YFP but not MSL8^{F720L}-YFP partially suppresses *msl8-4* pollen bursting and**

833 **germination when overexpressed in the *msl8-4* background.** (**A**) Pollen from the indicated lines

834 incubated in germination media for 6 hours and scored for combined germination and bursting categories

835 as in Fig. 4. Average of 3 to 6 experiments with N = 107 to 512 pollen per experiment. See

836 Supplementary Table 2 for statistical differences between groups. (**B**) Germination rate of pollen from the

837 indicated lines after incubation in germination media for 16 hours. Different letter groups indicate

838 significant (p < 0.05) differences between groups as determined by Tukey's post-hoc test following one-

839 way ANOVA. (**C**) Brightfield images of pollen from the indicated lines after incubation for 16 hours in liquid

840 germination media. Scale bars are 50 μm. (**A**, **B**) Error bars are mean ± SE.

841

842 **Figure 8. Effect of overexpressing MSL8-YFP variants from the *LAT52* promoter in the wild type**

843 **background on germination phenotypes.** (**A**) Quantitative reverse-transcription polymerase chain

844 reaction of endogenous *MSL8*, *MSL8-YFP*, and total *MSL8* transcripts relative to *ACTIN* in L*er*, *msl8-4*,

845 and *LAT52pMSL8-YFP* transgenic lines. (**B**) Pollen from the indicated lines incubated in germination

846 media for 6 hours and scored for combined germination and bursting categories as in Fig. 4. Averages

847 from 3 experiments with N = 82 to 250 pollen per experiment are presented. See Supplementary Table 3

848 for statistical differences between groups. (**C**) Germination rate of pollen from the indicated lines after

849 incubation in germination media for 16 hours. Averages of 3 experiments with N = 99 to 257 pollen per

850 experiment are presented. Different letter groups indicate significant (p < 0.05) differences between

851 groups as determined by Tukey's post-hoc test following one-way ANOVA. (**A-C**) Error bars are mean ±
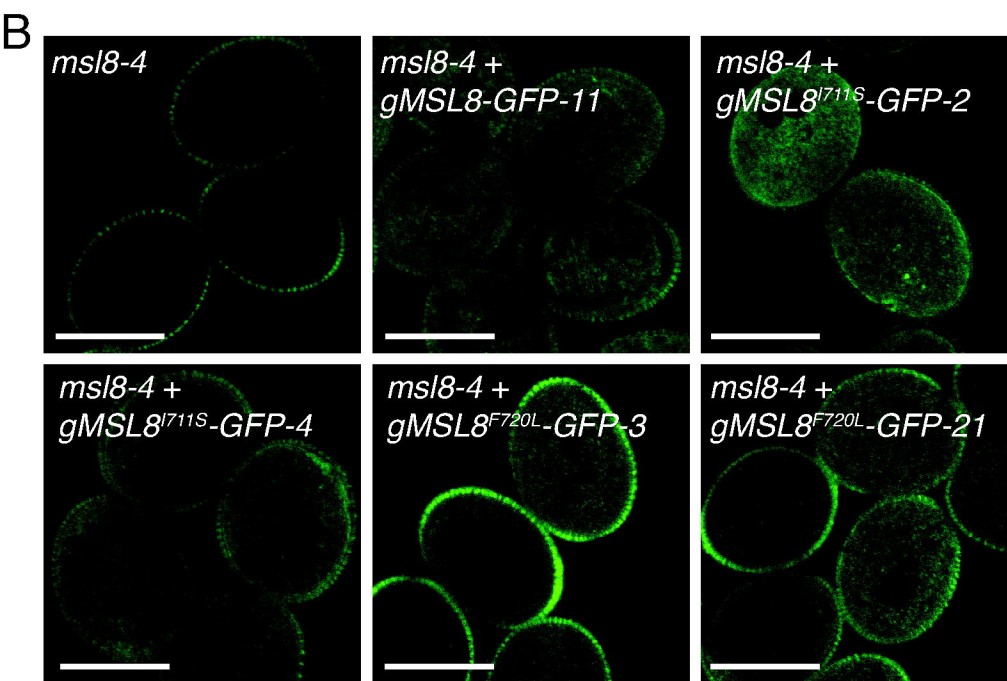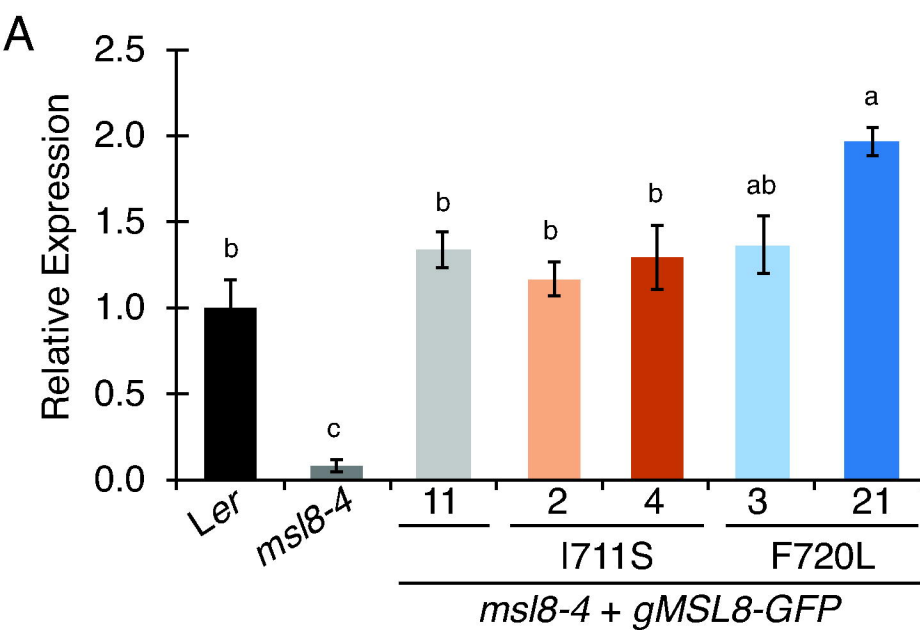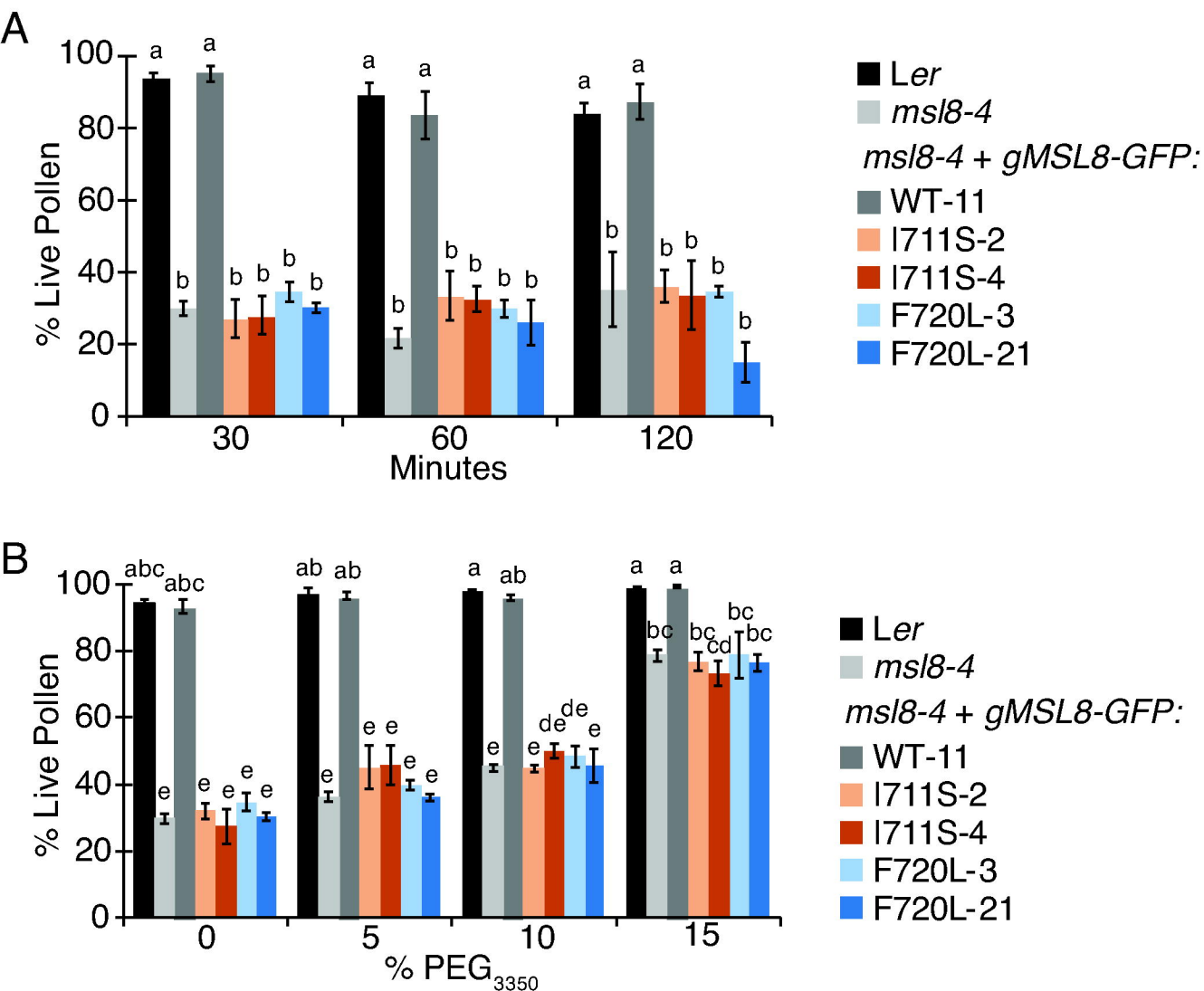
852 SE.

FIGURE 1

FIGURE 2

A

B
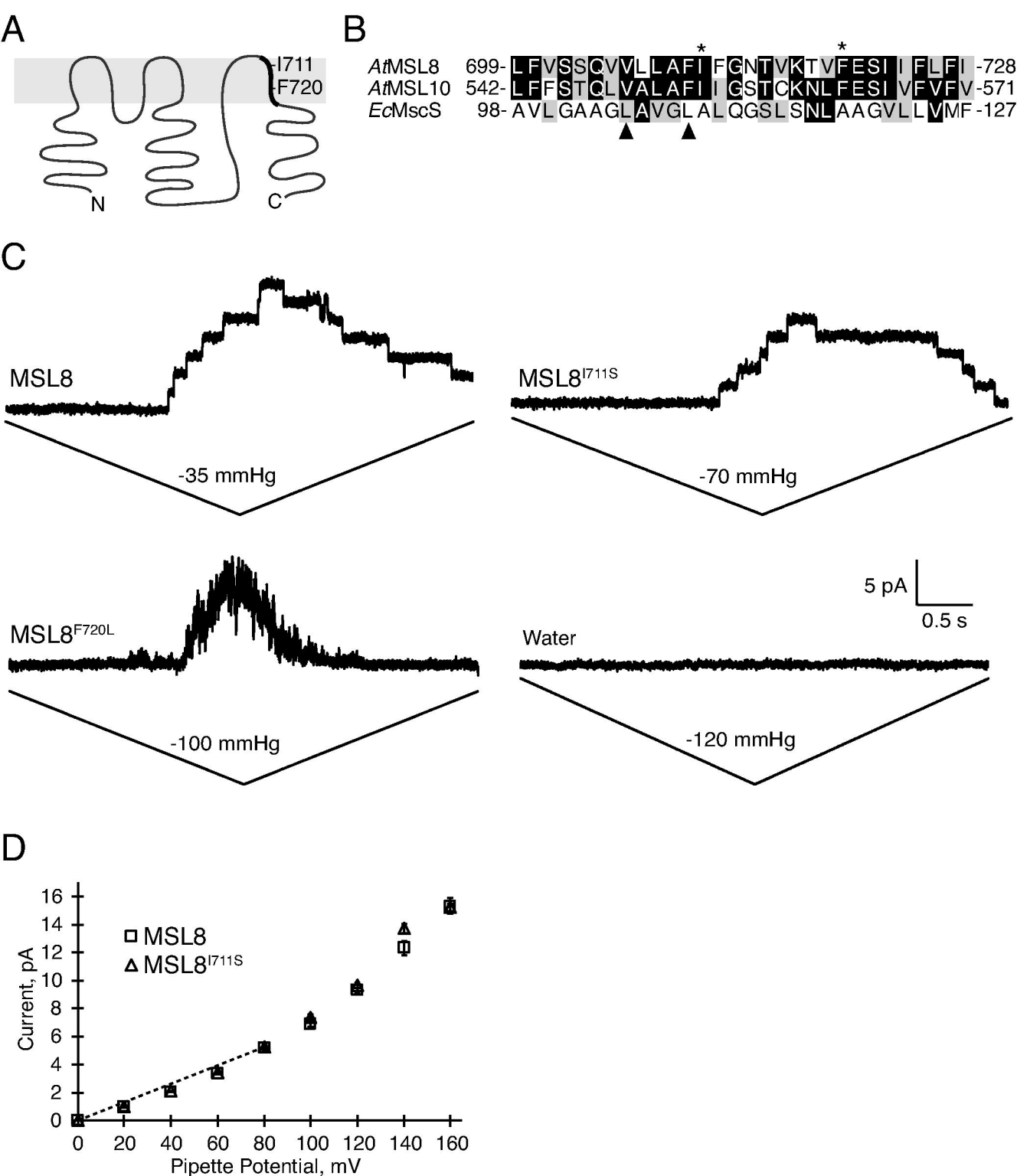
FIGURE 3

FIGURE 4

FIGURE 5

A

B

FIGURE 6

FIGURE 7

FIGURE 8